0026-895X/01/5906-1514–1522$3.00
MOLECULAR PHARMACOLOGY
Copyright © 2001 The American Society for Pharmacology and Experimental Therapeutics
Mol Pharmacol 59:1514–1522, 2001

Vol. 59, No. 6
825/908123
Printed in U.S.A.

Interactions between 3-(Trifluoromethyl)-3-(m-[^{125}I]iodophenyl)diazirine and Tetracaine, Phencyclidine, or Histrionicotoxin in the *Torpedo* Species Nicotinic Acetylcholine Receptor Ion Channel

MARTIN J. GALLAGHER,[1] DAVID C. CHIARA, and JONATHAN B. COHEN

Department of Neurobiology, Harvard Medical School, Boston, Massachusetts

Received January 17, 2000; accepted March 6, 2001

This paper is available online at http://molpharm.aspetjournals.org

ABSTRACT

3-(Trifluoromethyl)-3-(*m*-[^{125}I]iodophenyl)diazirine ([^{125}I]TID) and [^{3}H]tetracaine, an aromatic amine, are noncompetitive antagonists (NCAs) of the *Torpedo* species nicotinic acetylcholine receptor (nAChR), which have been shown by photoaffinity labeling to bind to a common site in the ion channel in the closed state. Although tetracaine and TID bind to the same site, the amine NCAs phencyclidine (PCP) and histrionicotoxin (HTX), which are also believed to bind within the ion channel, interact competitively with tetracaine but allosterically with TID. To better characterize drug interactions within the nAChR ion channel in the closed state, we identified the amino acids photoaffinity labeled by [^{125}I]TID in the presence of tetracaine, PCP, or HTX. In the absence of other drugs, [^{125}I]TID reacts with αLeu-251 (αM2-9) and αVal-255 (αM2-13) and the homologous residues in each of the other subunits. None of the NCAs shifted the sites of [^{125}I]TID labeling to other residues within the ion channel. Tetracaine inhibited [^{125}I]TID labeling of M2-9 and M2-13 without changing the relative ^{125}I incorporation at these positions, whereas PCP and HTX each altered the pattern of [^{125}I]TID incorporation at M2-9 and M2-13. These results indicate that tetracaine and TID bind in a mutually exclusive manner to a common site in the closed channel that is spatially separated from the binding sites for PCP and HTX.

The nicotinic acetylcholine receptor (nAChR) of vertebrate skeletal muscle and *Torpedo* species electric organ is a well characterized ligand-gated ion channel that exists in at least three interconvertible conformations: the resting (closed channel) state, the open channel state, and the agonist bound, nonconducting desensitized state (Hucho et al., 1996; Corringer et al., 2000). The nAChR is a pentamer of four homologous subunits ($\alpha_2\beta\gamma\delta$) with each subunit containing four hydrophobic transmembrane segments (M1-M4). The M2 segments of each subunit are α-helical and associate at the central axis of the nAChR to form the ion channel (Hucho et al., 1986; Imoto et al., 1988; Charnet et al., 1990; Revah et al., 1990; Imoto et al., 1991), with additional contributions from N-terminal residues of the M1 segments (Zhang and Karlin, 1997). The M3 and M4 segments contribute to the lipid-protein interface (Blanton and Cohen, 1994).

Many positively charged noncompetitive antagonists (NCAs), compounds that inhibit nAChR function by binding to sites other than the agonist binding site, bind within the lumen of the ion channel (for review, see Arias, 1998). Mutations in M2 affect the potencies of aromatic amine NCAs, including QX-222 (Charnet et al., 1990) and phencyclidine (Eaton et al., 2000), whereas mutations in M1 affect quinacrine potency (Tamamizu et al., 1995). For *Torpedo* species nAChRs equilibrated with agonist (i.e., in the desensitized state), the NCAs [^{3}H]chlorpromazine and [^{3}H]triphenylmethylphosphonium photoaffinity-labeled residues toward the N-terminal (cytoplasmic) end of each M2 segment (residues M2-6 and M2-9, with reference to the conserved Lys at the N-terminal end of each M2 segment) (Giraudat et al., 1986, 1987, 1989; Hucho et al., 1986; Revah et al., 1990), whereas [^{3}H]meproadifen mustard reacted with αGlu-262 (M2-20) at the extracellular end (Pedersen et al., 1992). In the absence of agonist (i.e., in the closed channel state), [^{3}H]tetracaine was specifically photoincorporated into amino acids in the middle of each M2 segment (M2-9 and M2-13) (Gallagher and Cohen, 1999). In contrast, in the open channel state,

This research was supported in part by U.S. Public Health Service Grant NS19522 and by an award in Structural Neurobiology from the Keck Foundation.

[1] Present address: Department of Neurology, Washington University School of Medicine, St. Louis, Missouri.

ABBREVIATIONS: nAChR, nicotinic acetylcholine receptor; NCA, noncompetitive antagonist; TID, 3-(trifluoromethyl)-3-(*m*-iodophenyl)diazirine; HTX, histrionicotoxin; PCP, phencyclidine; ACh, acetylcholine; EndoLys-C, endoproteinase Lys-C; PAGE, polyacrylamide gel electrophoresis; 1-AP, 1-azidopyrene; HPLC, high-performance liquid chromatography; PTH, phenylthiohydantoin; ANOVA, analysis of variance.

[^{3}H]quinacrine azide photolabeled amino acids within the M1 segment (DiPaola et al., 1990). Affinity labeling studies also have shown that uncharged NCAs bind within the nAChR ion channel. In the absence of agonist, [^{125}I] 3-(trifluoromethyl)-3-(*m*-iodophenyl)diazirine (TID) specifically labeled the same amino acids as [^{3}H]tetracaine (M2-9 and -13 of each subunit), whereas in the desensitized state [^{125}I]TID labeled residues deeper in the pore (M2-2 and -6) (White and Cohen, 1992). In the absence of agonist, [^{3}H]diazofluorene selectively labeled amino acids in δ-subunit (δM2-9 and -13) and in the β-subunit (βM2-13), with the labeling in the desensitized state also shifted to residues closer to the cytoplasmic end (δM2-6, βM2-9 and -10) (Blanton et al., 1998).

[^{3}H]Histrionicotoxin (HTX) and [^{3}H]phencyclidine (PCP) are well characterized NCAs that have each been shown to bind reversibly to a single site in the *Torpedo* species nAChR (Heidmann et al., 1983). [^{3}H]HTX binds with similar high affinity (K_D = ~0.3 μM) to nAChRs in the resting and desensitized states, whereas [^{3}H]PCP binds with K_D values of 1 μM to the desensitized state and ~6 μM to the resting state. They serve as useful probes of the NCA site in the nAChR because they bind relatively weakly to the ACh sites, and they seem to interact with fewer low-affinity sites in the *Torpedo* species nicotinic postsynaptic membrane than other, more lipophilic NCAs. Although these compounds are assumed to bind within the ion channel, the binding site for neither NCA has been directly identified by affinity labeling. HTX and PCP bind in a mutually exclusive manner with each other and with other aromatic amine NCAs. In the desensitized state, PCP and HTX bind competitively with [^{3}H]meproadifen mustard (Dreyer et al., 1986), a compound that seems to bind at the extracellular end of the ion channel domain (M2-20), and also with [^{3}H]chorpromazine (Heidmann et al., 1983), a compound that binds lower in the channel domain (M2-6 and -9). In the absence of agonist, PCP and HTX bind competitively with [^{3}H]tetracaine (Middleton et al., 1999), a result suggesting that the three ligands bind in a mutually exclusive manner to a common site at M2-9 and M2-13. However, in the absence of agonist, PCP and HTX interact allosterically with TID, a compound that binds to the same site as [^{3}H]tetracaine. When evaluated at the level of nAChR subunits, PCP binding to its high-affinity site inhibited specific [^{125}I]TID photoincorporation in the α-, β-, and γ-subunits by only 20 to 30%, whereas it increased labeling in the δ-subunit (White and Cohen, 1988; Ryan et al., 2001). TID at 100 μM did not effect [^{3}H]PCP binding, and it increased the K_D value of [^{3}H]HTX only 5-fold (White et al., 1991).

To further characterize drug interactions within the ion channel, we have mapped, at the amino acid level, the binding site for [^{125}I]TID in the ion channel in the presence of tetracaine, PCP, or HTX. We wanted to test the hypothesis that tetracaine would reduce [^{125}I]TID photoincorporation in the M2 ion channel domain in a manner consistent with mutually exclusive binding. We also wanted to determine whether the binding site for [^{125}I]TID in the ion channel was shifted in the presence of either HTX or PCP.

Experimental Procedures

Materials. nAChR-rich membranes were isolated from electric organs of *Torpedo* species (Winkler Enterprises, San Pedro, CA) as described elsewhere (Pedersen et al., 1986). The membranes used contained 1 to 2 nmol of [^{3}H]ACh binding sites per milligram of protein. Endoproteinase Lys-C (EndoLys-C) was from Roche Molecular Biochemicals (Indianapolis, IN), 1-tosylamido-2-phenylethychlormethyketone-treated trypsin was from Worthington Biochemical (Freehold, NJ), and *Staphylococcus aureus* glutamyl endopeptidase (V8 protease) was from ICN Biomedical Inc. (Cosa Mesa, CA). Prestained low molecular mass gel standards were from Life Technologies (Gaithersburg, MD): ovalbumin (43 kDa), carbonic anhydrase (29 kDa), β-lactoglobulin (18 kDa), lysozyme (14 kDa), bovine trypsin inhibitor (6 kDa), and insulin (2.8 kDa). Genapol C-100 (10%) and trifluoroacetic acid were from Pierce (Rockford, IL). 1-Azidopyrene was bought from Molecular Probes (Eugene, OR). [^{125}I]TID (10 Ci/mmol) was obtained from Amersham Pharmacia Biotech (Piscataway, NJ), and [^{3}H]tetracaine (48 Ci/mmol) was prepared by tritium reduction (PerkinElmer Life Science Products, Boston, MA) of 3,5-dibromotetracaine as described previously (Gallagher and Cohen, 1999). PCP was from Applied Science (State College, PA) and HTX was kindly provided by Dr. Y. Kishi (Harvard University, Cambridge, MA). Nonradioactive TID was a gift from Dr. S. Husain (Massachusetts General Hospital, Boston, MA) and was repurified by silica gel chromatography (100% hexane elution) and stored in 100% ethanol after the hexane was removed by rotary evaporation. Purity and concentration of the TID was assessed by silica thin-layer chromatography and UV absorption at 365 nm (Brunner and Semenza, 1981). Structures of the drugs are shown in Fig. 1.

[^{3}H]Tetracaine Binding. The equilibrium binding of [^{3}H]tetracaine (10 nM) to nAChR-rich membranes in *Torpedo* species physiological saline (250 mM NaCl, 5 mM KCl, 3 mM $CaCl_2$, 2 mM $MgCl_2$, 5 mM NaPi, pH 7.0) was measured by a filtration assay (Middleton et al., 1999). Membrane suspensions (400 nM ACh sites) were incubated in the dark for 30 min at room temperature with [^{3}H]tetracaine and various concentrations of nonradioactive TID before filtration, and nonspecific binding was defined as the amount of [^{3}H]tetracaine bound in the presence of 100 μM nonradioactive tetracaine.

[^{125}I]TID Photolabeling. Photolabeling on an analytical scale was used to quantify [^{125}I]TID photoincorporation into nAChR subunits in the presence of tetracaine at concentrations from 1 μM to 1

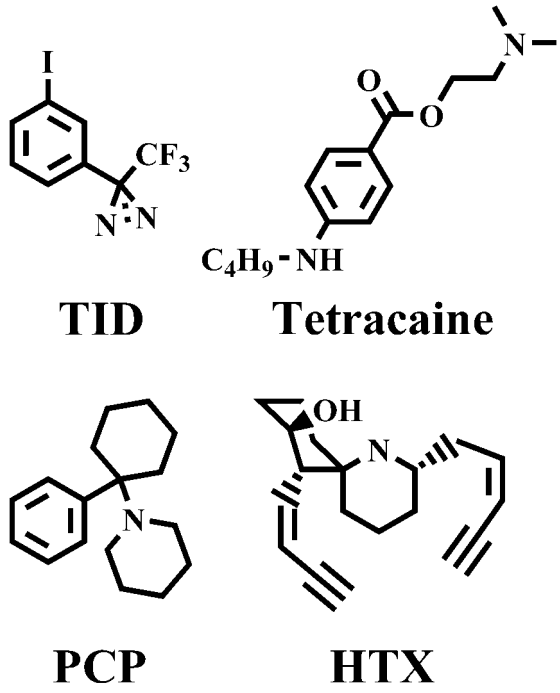

Fig. 1. Structures of nAChR noncompetitive antagonists.

mM. nAChR-rich membranes (100 μl, 2 mg of protein/ml) were incubated in the dark in microtiter plates with [^{125}I]TID (6.5 μM) and nonradioactive tetracaine for 30 min. The suspensions were then photolyzed for 30 min at 365 nm (model EB-280C; Spectroline, Westbury, NY) at a distance of 6 cm. Sample buffer was then added directly to the membrane suspensions, which were then separated by SDS-PAGE gel on an 8% acrylamide gel. The polypeptides on the gel were visualized by Coomassie blue stain, and the [^{125}I]TID incorporation in the gel was detected by autoradiography or by use of a Storm PhosphorImager (Molecular Dynamics, Sunnyvale, CA). The nAChR γ-subunit ^{125}I incorporation was quantified using the ImageQuaNT software, with background levels calculated locally.

Preparative [^{125}I]TID photolabeling was performed essentially as described previously (White and Cohen, 1992; Blanton and Cohen, 1994). nAChR-rich membranes (5–7 mg at 2 mg of protein/ml in *Torpedo* species physiological saline) were equilibrated for 30 min with 6.5 μM [^{125}I]TID and in the absence or presence of an amine NCA and then photolyzed at 365 nm under one of two conditions. The samples were either photolyzed for 30 min in open glass containers at a distance of 6 cm (White and Cohen, 1992) or irradiated in closed glass vials for 10 min at a distance of 1 cm (Blanton and Cohen, 1994). Because the closed vials more effectively contained volatilized [^{125}I]TID and because the pattern of [^{125}I]TID labeling within the nAChR M2 segments did not vary between the two methods, the closed vial method was used routinely.

To facilitate the isolation of subunits and proteolytic fragments, the [^{125}I]TID-labeled membranes were further photolabeled with the fluorescent, hydrophobic probe 1-azidopyrene (1-AP) as described previously (Blanton and Cohen, 1994). The membrane suspensions were then pelleted, resuspended in sample buffer, and electrophoresed on 1.5-mm thick slab gels.

After electrophoresis, the unstained gels were illuminated on a 365-nm UV light box and the nAChR subunits were visualized by 1-AP fluorescence. The bands containing the nAChR β-, γ-, and δ-subunits were excised from the gels, diced, and eluted in 10 ml of elution buffer (0.1 M NH_4HCO_3/0.1% SDS, pH 7.8), whereas the α-subunit was subjected to an "in-gel" *S. aureus* glutamyl endopeptidase (V8 protease) digestion (Cleveland et al., 1977; Pedersen et al., 1986). The α-subunit fragment of ~20 kDa (αV8-20) was visualized by 1-AP fluorescence (Blanton and Cohen, 1992), excised from the gel, and eluted as described above.

After 4 days of elution, the samples were concentrated in Centriprep-10 (αV8-20) or Centriprep-30 (β-,γ-, and δ-subunits) Microconcentrators (Amicon, Beverly, MA) to approximately 400 μl and precipitated in 1.6 ml of acetone at −20°C to remove excess SDS. The αV8-20 fragments and δ-subunits were resuspended in 125 μl of 15 mM Tris, pH 8.1/0.1% SDS, and the β-subunits were resuspended in 150 μl of 0.1 M NH_4HCO_3, pH 7.8/0.5% Genapol/0.02% SDS. Protein concentrations of the samples were measured using a bicinchoninic acid-based protein assay (Micro BCA Protein Assay; Pierce), and the amount of [^{125}I]TID incorporation into each subunit was determined by gamma counting.

Proteolytic Digestion and Fragment Purification. The goal in these experiments was to characterize the effect of noncompetitive antagonists on [^{125}I]TID incorporation into the M2 hydrophobic segments. Therefore, the techniques used to generate the [^{125}I]TID-labeled fragments used the digestion conditions previously optimized (White and Cohen, 1992; Gallagher and Cohen, 1999) to produce fragments beginning at the N termini of the M2 segments. Briefly, solutions (1 mg of protein/ml) of αV8-20 fragments and intact δ-subunit in 15 mM Tris, pH 8.1, 0.1% SDS were digested for 3 to 5 days with 4 U/ml of EndoLys-C, whereas the β-subunit (approximately 1 mg/ml) in 100 mM NH_4HCO_3, pH 7.8/0.02% SDS/0.5% Genapol C-100 was digested with trypsin [3:2 (w/w), protein/trypsin] for 3 to 7 days. The αV8-20 and δ-subunit digests were fractionated on 16.5% T/3% C Tricine gels (Schagger and von Jagow, 1987), and the β-subunit digests were resolved on a 16.5%T/6%C Tricine gel to obtain higher resolution. Regions of the gels that were expected to contain peptides beginning at the N termini of the M2 segments were identified based upon the migration of prestained molecular mass markers and the pattern of 1-AP fluorescence (Gallagher and Cohen, 1999). Nonfluorescent regions at 8 and 7 kDa were excised from the αV8-20 and β-subunit digests, respectively, and a fluorescent band at 10 kDa was excised from the δ-subunit digest. Material was eluted from the bands, and the eluates were concentrated to 0.3 ml in Centricon-3 microconcentrators (Amicon). The concentrates were then fractionated by reversed phase HPLC as a second purification step that also removed the majority of the SDS. Based upon the distribution of ^{125}I, fractions were pooled, dried by vacuum centrifugation, and then resuspended in 25 μl of 100 mM NH_4HCO_3/0.05% SDS.

Sequence Analysis. The purified samples were applied to chemically modified glass fiber filters (Beckman, Palo Alto, CA) that were first washed with distilled water and methanol to remove impurities that inhibit binding of hydrophobic peptides. The purified peptides were fixed to the filters by delivery of gas trifluoroacetic acid for 4 min and then the SDS was removed from the filters by washing them for 5 min with ethyl acetate. The peptides were sequenced on an ABI 477 protein sequencer (Applied Biosystems, Foster City, CA) with gas phase sequencing cycles. During Edman degradation, two thirds of each sample was sent to a fraction collector for ^{125}I gamma counting and one third was injected on an amino acid analyzer (ABI 120A) to identify the PTH-amino acid. Picomoles of each PTH amino acid were calculated from the peak height on the analyzer chromatogram (ABI 610A Data Analysis Program version 1.2.1). The background-subtracted yields (excluding serines and cysteines) of each sequencing cycle were fit to the equation $I(n) = I_0 \times R^n$, where $I(n)$ is picomoles of PTH amino acid at cycle n, I_0 is the initial peptide quantity in picomoles, and R is the sequencer repetitive yield. The efficiency of [^{125}I]TID incorporation into residue n, expressed as cpm_n per picomole (I_n), was calculated by $[cpm_n - cpm_{n-1}]/2 \times I_n$ with the factor of 2 in the denominator because at each cycle the volume counted was twice the volume injected into the amino acid analyzer. We employed a single factor ANOVA test (Microsoft Excel) to determine whether tetracaine, PCP, or HTX induced significant differences in the percentage of change of [^{125}I]TID labeling efficiencies of αM2-9, αM2-13, δM2-9, and δM2-13. We also used a two-tailed t test (Microsoft Excel; Microsoft, Redmond, WA) to determine whether there were significant differences in the ratios of ^{125}I incorporation in M2-9 and M2-13 within a single subunit.

Results

In initial experiments, we examined the effects of tetracaine on the photoincorporation of [^{125}I]TID into nAChR-rich membranes as well as the effects of TID on the reversible binding of [^{3}H]tetracaine (Fig. 2). nAChR-rich membranes (1.5 μM ACh sites) were equilibrated with 6.5 μM [^{125}I]TID and various concentrations of tetracaine, and after photolysis the polypeptides were separated by SDS-PAGE. The gel was stained with Coomassie blue to allow identification of nAChR subunits and to verify that the lanes contained similar amounts of protein, and the distribution of ^{125}I was determined by PhosphorImaging (Fig. 2A). Consistent with previous results (White and Cohen, 1988), [^{125}I]TID was photoincorporated into each nAChR subunit, with the γ-subunit labeled most efficiently. (A prominently labeled γ-subunit fragment migrating near 45 kDa was also noted.) Tetracaine reduced ^{125}I incorporation in each nAChR subunit in a dose-dependent manner, whereas it had no effect on the ^{125}I incorporation in the α-subunit of the Na^+/K^+-ATPase, which was labeled at lower efficiency than any of the nAChR subunits in the absence of tetracaine. When the concentration dependence of tetracaine inhibition of ^{125}I incorporation in

nAChR γ-subunit was quantified (Fig. 2B), the data were fit by a single site model with an IC_{50} value of 3 μM, and tetracaine reduced subunit labeling by ~90%. The IC_{50} value was the same as for its inhibition of [^{3}H]HTX binding and, as expected, for tetracaine binding to its high-affinity site in the nAChR M2 ion channel domain (Gallagher and Cohen, 1999; Middleton et al., 1999). Nonradioactive TID also inhibited the reversible binding of [^{3}H]tetracaine (Fig. 2B) with a concentration dependence characterized by an IC_{50} value of 3 μM. At high concentrations, TID inhibited at least 95% of specifically bound [^{3}H]tetracaine. These results contrasted with the interactions between TID and PCP or HTX (White and Cohen, 1988; White et al., 1991). TID did not inhibit [^{3}H]PCP binding in the absence of agonist, and PCP reduced [^{125}I]TID photolabeling of nAChR γ-subunit by less than 30%.

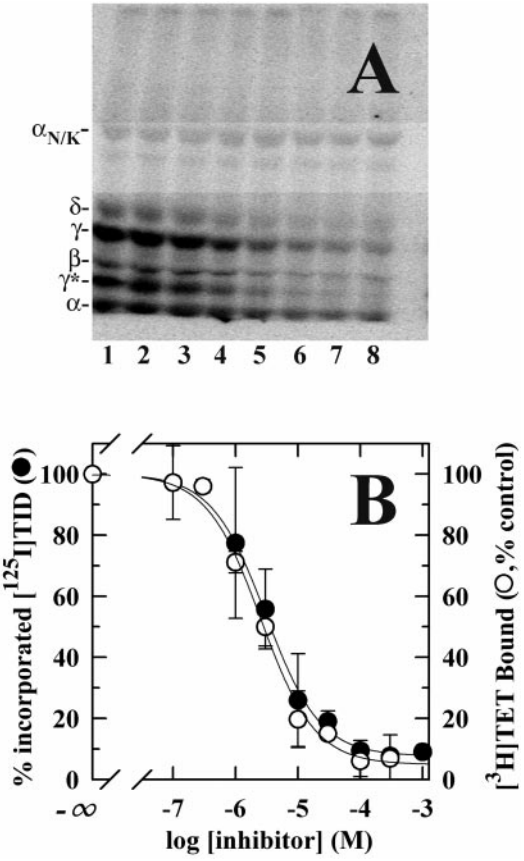

Fig. 2. Mutual inhibition of tetracaine and TID binding to the nAChR. A, suspensions of nAChR-rich membranes (2 mg/ml) were equilibrated with 6.5 μM [^{125}I]TID and tetracaine (lanes 1–8: 0, 1, 3, 10, 30, 100, 300, 1000 μM) and then photolyzed at 365 nm. The membrane polypeptides were then fractionated by SDS-PAGE and visualized by Coomassie blue staining (data not shown). ^{125}I incorporation in the polypeptides was visualized by phosphoimaging. B, concentration dependence of tetracaine inhibition of [^{125}I]TID incorporation into nAChR γ-subunit (●) and of TID inhibition of the equilibrium binding of [^{3}H]tetracaine (○). For the experiment in A and two similar experiments ^{125}I incorporation in the nAChR γ-subunit was quantified using ImageQuaNT software (●, mean ± S.D.). The concentration dependence of tetracaine inhibition was fit to a single-site model with an IC_{50} value of 3.1 ± 0.2 μM and a maximal inhibition of 92 ± 1%. The equilibrium binding of [^{3}H]tetracaine (10 nM) to nAChR-rich membranes (200 nM nAChR) was determined by a filtration assay, with the nonspecific binding defined as the amount of ^{3}H retained in the presence of 100 μM tetracaine. The percentage of specifically bound [^{3}H]tetracaine [$f(x)$] was calculated at each concentration of TID (x), and the data points are the average and standard deviations of three experiments. The concentration dependence of inhibition of [^{3}H]tetracaine binding (or [^{125}I]TID photolabeling of γ-subunit) was fit to a single-site model $f(x) = (100 - A) / [1 + (x / IC_{50})] + A$, with the IC_{50} value and A (the residual binding or subunit photolabeling) as adjustable parameters. TID inhibits [^{3}H]tetracaine binding with an IC_{50} value of 2.4 ± 0.4 μM and a maximal inhibition of 95 ± 3%.

Mapping [^{125}I]TID Photoincorporation in nAChR M2 Segments. Suspensions of nAChR-rich membranes (5 mg, 2 mg/ml) were incubated with [^{125}I]TID in the absence of additional ligand and in the presence of 30 μM tetracaine, 50 μM PCP, or 30 μM HTX. The suspensions were photolyzed, and the nAChR β-, γ-, and δ-subunits as well as the αV8-20 fragment were isolated as described under *Experimental Procedures*. Typically, 100 to 200 μg of each subunit or of αV8-20 were recovered. Based upon previous studies (Gallagher and Cohen, 1999), digestion of αV8-20 or δ-subunit with EndoLys-C would produce fragments of ~10 kDa beginning at the N termini of the M2 segments that can be purified by Tricine SDS-PAGE and HPLC. For the β-subunit, digestion with trypsin produces a similar fragment of ~7 kDa (White and Cohen, 1992). For nAChRs labeled with [^{125}I]TID in the absence or presence of amine NCAs, we also found that when aliquots of the subunit digests were fractionated by Tricine SDS-PAGE, for both αV8-20 and the δ-subunit, the predominant [^{125}I]TID-labeled fragments had mobilities of ~10 kDa (Fig. 3). The presence of tetracaine or HTX, but not PCP, reduced ^{125}I incorporation in the α- and δ-subunit fragments without the appearance of any novel labeled bands. Trypsin digestion of labeled β-subunit produced a specifically labeled band of ~7 kDa (data not shown). The bulk of these digests was fractionated by Tricine SDS-PAGE on a preparative scale, and the material eluted from the gel bands was further purified by reversed phase HPLC (Fig. 4), from which the fractions containing the peak of ^{125}I were pooled for N-terminal sequence analysis.

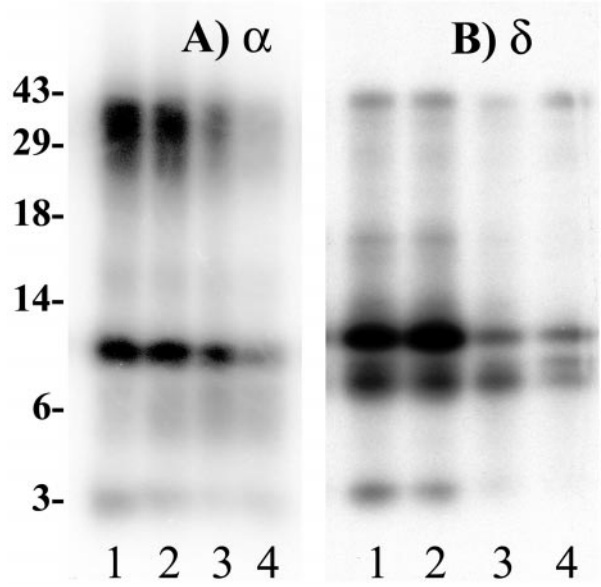

Fig. 3. Products of EndoLys-C digestion of [^{125}I]TID-labeled nAChR subunits resolved by Tricine SDS-PAGE. αV8-20 fragments (A) and δ-subunits (B) from nAChRs labeled with [^{125}I]TID in the absence of additional ligand (lane 1), or in the presence of 50 μM PCP (lane 2), or 30 μM HTX (lane 3), or 30 μM tetracaine (lane 4) were digested with EndoLys-C as described under *Experimental Procedures*, and aliquots (8%) of each digestion mixture were run on an analytical Tricine SDS-PAGE gel. Shown here is an autoradiogram of the gel (1-week exposure) along with the migration distances of the prestained molecular mass markers.

[^{125}I]TID Photoincorporation in the Presence of Tetracaine. Subunit fragments were isolated from nAChRs labeled with [^{125}I]TID in the absence and presence of 30 μM tetracaine. Sequence analysis of the purified α-, β-, and δ-subunit fragments each revealed a single sequence beginning at the N terminus of the M2 segments (Fig. 5). For each of the subunit fragments isolated from nAChRs that were labeled in the absence of tetracaine, there was ^{125}I release at cycles 9 and 13 of Edman degradation, corresponding to incorporation at αLeu-251 (αM2-9) and αVal-255 (αM2-13), βLeu-257 (βM2-9), and βLeu-261 (βM2-13), or δLeu-265 (δM2-9) and δLeu-269 (δM2-13). These results agree with the previous characterizations of amino acids in the nAChR M2 domain that are specifically labeled by [^{125}I]TID (Blanton and Cohen, 1992; White and Cohen, 1992). As was seen previously, within β-subunit [^{125}I]TID was incorporated with greater efficiency at βM2-9 than at βM2-13, whereas for α- and δ-subunits, the labeling at M2-13 was more prominent. Sequence analysis of the fragments isolated from nAChRs labeled in the presence of tetracaine similarly were characterized by ^{125}I release in the M2 segments only at positions 9 and 13 (Fig. 5), but for each subunit the efficiency of incorporation at M2-9 and M2-13 was reduced by 90% (Table 1A). When the data were combined from multiple labeling experiments, tetracaine at 30 μM reduced the efficiency of [^{125}I]TID labeling of αM2-9, αM2-13, βM2–9, βM2-13, δM2-9, and δM2-13 by 88 $\pm$ 4% (Table 2). There was no significant difference in the relative reduction of labeling in any of the residues (ANOVA, $p = 0.76$). Furthermore, there were no significant differences in the ratios of ^{125}I incorporation in δM2-9 to δM2-13 ($p = 0.77$) or αM2-9 to αM2-13 ($p = 0.89$) in

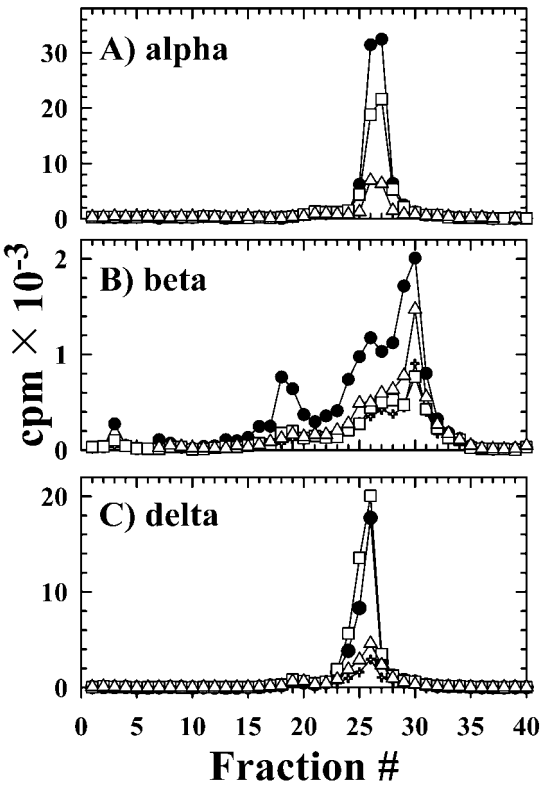

Fig. 4. Purification by reversed phase HPLC of [^{125}I]TID-labeled fragments from proteolytic digests of nAChR subunits. nAChR-rich membranes were photolabeled with 6.5 μM [^{125}I]TID in the absence of other NCAs (●) or in the presence of 30 μM tetracaine (+), 50 μM PCP (□), or 30 μM HTX (△). EndoLys-C digests of [^{125}I]TID-labeled αV8-20 and δ-subunits and trypsin digests of labeled β-subunits were fractionated by Tricine SDS-PAGE. The bands of 8 to 10 kDa expected to contain fragments beginning at the N termini of M2 were excised and eluted as described under *Experimental Procedures* and then fractionated by reversed phase HPLC (Brownlee C-4 column, 0.2 × 10 cm) with the elution gradient increasing linearly from 25% to 100% solvent B (60% acetonitrile, 40% isopropanol, 0.05% trifluoroacetic acid) in 80 min. (Solvent A was 0.08% trifluoroacetic acid.) Flow was 0.2 ml/min, fractions were collected every 2.5 min, and total ^{125}I cpm in each of the fractions was determined by gamma counting. Each of the profiles shown for a given subunit is from the same labeling experiment, but the data for the α-subunit are from different labeling experiment than the data for the β- and δ-subunits. There was no labeling experiment in which the effect of tetracaine on [^{125}I]TID-labeling in α-subunit was characterized at the same time as PCP and HTX, so for the α-subunit, no data are included for tetracaine. For the α-subunit, fractions 26 and 27 were pooled for sequence analysis, whereas for β- and δ-subunits, fractions 28 to 31 and 25 to 26 were pooled. ^{125}I cpm recovered in the pooled fractions: α-subunit (A) (control, 63,900; +PCP, 40,000; +HTX, 13,300); β-subunit (B) (control, 5,650; +tetracaine, 2,120; +PCP, 2,190; +HTX, 3,440); δ-subunit (C) (control, 26,090; +tetracaine, 4,540; +PCP, 33,600; +HTX, 7,500).

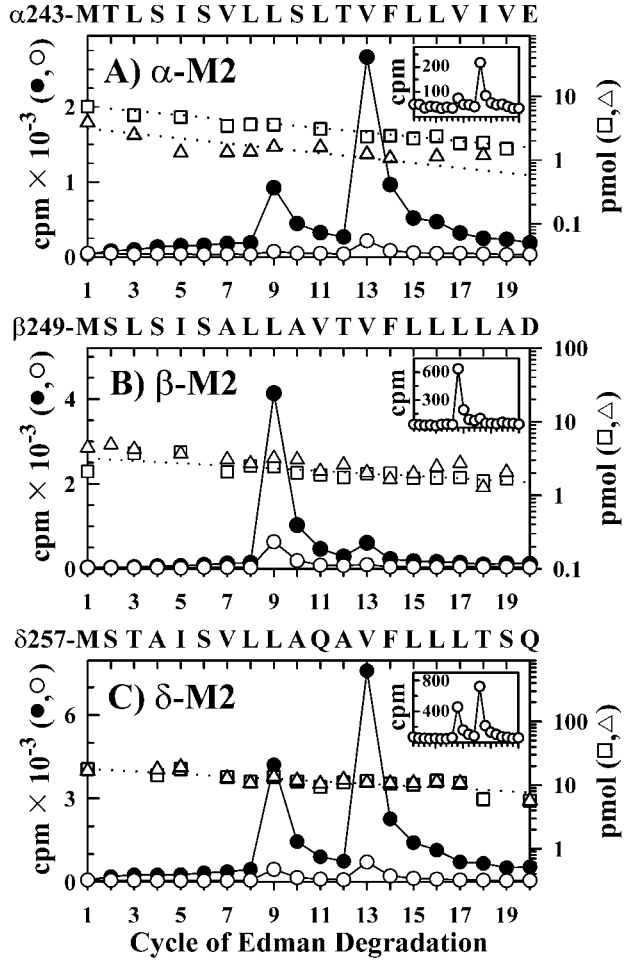

Fig. 5. Effect of tetracaine on [^{125}I]TID incorporation within the M2 ion channel domain. A–C, ^{125}I (●, ○) and picomoles of residues (□, △) released during N-terminal sequencing of α-, β-, and δ-subunit fragments isolated by SDS-PAGE and reversed phase HPLC from nAChRs photoincorporated with [^{125}I]TID in the absence (●, □) and presence (●, △) of 30 μM tetracaine. All data are from a single labeling experiment. For each subunit, the only sequence detected began at the amino terminus of the M2 segment, shown at the top of each panel. The initial (I_o) and repetitive (R) yields of for each sample as well as the efficiency of incorporation into M2-9 and M2-13 are listed in the Table 1A. Insets, ^{125}I release profiles for the samples labeled in the presence of tetracaine were plotted on an expanded scale to better visualize the pattern of ^{125}I release.

the presence and absence of tetracaine. Thus, in the presence of tetracaine there was no evidence that [^{125}I]TID was shifted within the M2 ion channel domain to be in contact with amino acids other than M2-9 and M2-13, and the proportionate reduction of ^{125}I incorporation at all amino acids was consistent with mutually exclusive binding of either [^{125}I]TID or tetracaine.

[^{125}I]TID Photoincorporation in the Presence of PCP and HTX. nAChR-rich membranes were incubated with [^{125}I]TID in the absence of additional ligand and in the presence of either 50 μM PCP or 30 μM HTX. These concentrations of NCAs were chosen to maximize binding to the high-affinity site while avoiding binding to the agonist site or to other low-affinity binding sites (Heidmann et al., 1983). At these concentrations, PCP and HTX each caused maximal change in of [^{125}I]TID incorporation into the nAChR as determined at the level of individual subunits (White and Cohen, 1988). The suspensions were photolyzed, and the nAChR β-, γ-, and δ-subunits as well as the αV8-20 fragment were isolated. HTX reduced ^{125}I incorporation in αV8-20 by 80%, β-subunit by 70%, γ-subunit by 80%, and δ-subunit by 50%. PCP reduced labeling in the β-subunit by 20% and in the αV8-20 fragment by 60%, but it increased labeling in the δ-subunit by 20% and in the γ-subunit by 10%. These results were generally consistent with previous studies (White and Cohen, 1988). Fragments of the α-, β-, and δ-subunits that begin at the N termini of the M2 segments were generated, purified, and sequenced (Figs. 6 and 7). For the fragments isolated from nAChRs labeled in the presence of PCP (Fig. 6) or HTX (Fig. 7) there were peaks of ^{125}I release in cycles 9 and 13, without the appearance of any novel labeled amino acids within the M2 segments. In contrast to tetracaine, PCP altered ^{125}I incorporation into each residue differently (Fig. 6; Table 1B). The addition of 50 μM PCP *enhanced* the labeling of δM2-9 by 2-fold while reducing incorporation by 30 to 70% at the equivalent position in αM2 and βM2. In the presence of PCP there was no change in the labeling of δM2-13. When the data were combined from multiple experiments (Table 2) these changes in the [^{125}I]TID labeling pattern were statistically significant by ANOVA ($p = 0.007$). Furthermore, the ratios of ^{125}I labeling in M2-9 to M2-13 were significantly different in the presence and absence of PCP in both δM2 ($p < 0.001$) as well as αM2 ($p = 0.015$).

HTX (30 μM) reduced [^{125}I]TID incorporation into each M2 residue (Fig. 7), with the percentage reduction differing among the labeled residues: αM2-9 (93%), αM2-13 (94%), βM2-9 (54%), δM2-9 (67%), and δM2-13 (86%) (Table 1C). When the results from independent experiments were averaged (Table 2), the variances in percentage of reduction of ^{125}I incorporation (Table 1) were such that there was no

TABLE 1

Summary of sequence analyses of nAChR subunit fragments

For each of the sequencing runs in Figs. 5–7, the initial (I_o) and repetitive (R) yields were calculated by fitting the pmol [$I(n)$] of PTH-amino acid detected at each cycle (n) of Edman degradation to the equation, $I(n) = I_oR^n$. Also tabulated are the ^{125}I cpm loaded and remaining on the filters after 20 cycles of Edman degradation. The efficiency of incorporation (^{125}I cpm/pmol) into residues M2-9 and M2-13 were calculated as described under *Experimental Procedures*.

		I_0	R	cpm Loaded	cpm Filter	cpm/pmol		Ratio 9:13
						9	13	
A Tetracaine								
α-M2	NA	6.9 ± 0.3	93 ± 1	23,300	10,700	108	480	0.22
	TET	3.4 ± 0.5	92 ± 2	4,600	480	12	82	0.16
β-M2	NA	3.3 ± 0.4	96 ± 1	21,100	7,300	862	82	11
	TET	4.9 ± 0.3	94 ± 1	8,600	3,700	103	5	21
δ-M2	NA	19 ± 1	96 ± 1	67,700	24,800	150	330	0.46
	TET	19 ± 1	96 ± 1	6,400	3,100	15	30	0.50
B Phencyclidine								
α-M2	NA	31 ± 3	93 ± 1	38,500	15,200	14	62	0.23
	PCP	59 ± 4	90 ± 1	19,100	7,300	4	33	0.11
β-M2	NA	11 ± 1	88 ± 1	6,500	1,700	35	11	3.1
	PCP	2.5 ± 0.5	91 ± 3	1,800	700	23	16	1.4
δ-M2	NA	32 ± 2	96 ± 1	50,400	13,200	35	73	0.47
	PCP	37 ± 4	96 ± 2	56,700	3,800	81	53	1.5
C Histrionicotoxin								
α-M2	NA	31 ± 3	93 ± 1	38,500	15,200	14	62	0.23
	HTX	59 ± 6	94 ± 1	12,400	ND	0.4	3.8	0.12
β-M2	NA	11 ± 1	88 ± 1	6,500	1,700	35	11	3.1
	HTX	11 ± 1	89 ± 2	2,600	1,100	16	4	4.0
δ-M2	NA	37 ± 4	95 ± 1	49,200	12,200	40	81	0.50
	HTX	50 ± 3	94 ± 1	1,900	2,000	13	11	1.1

TABLE 2

Effects of NCAs on [^{125}I]TID incorporation in M2-9 and M2-13 of nAChR α- and δ-subunits: averages from of multiple labeling experiments

The efficiency of [^{125}I]TID incorporation at M2-9 and M2-13 in the absence of additional ligand (control) or in the presence of tetracaine, PCP, or HTX was calculated as described under *Experimental Procedures*. From the data for each labeling experiment the ratios of labeling at M2-9 and M2-13 were calculated, and the averages of the ratios were determined for all experiments. In addition, for each position the percentage of reduction of labeling was determined from the efficiency of [^{125}I]TID incorporation in the presence of NCA relative to control. The values tabulated are the averages of different labeling experiments ± the standard deviations. The number of labeling experiments used in the determinations is given in parentheses.

	Ratio δM2-9/δM2-13	% Reduction δM2-9	% Reduction δM2-13	Ratio αM2-9/αM2-13	% Reduction αM2-9	% Reduction αM2-13
Control	0.49 ± 0.05 (8)			0.34 ± 0.12 (7)		
Tetracaine	0.48 ± 0.04 (3)	89 ± 3 (3)	89 ± 5 (3)	0.31 ± 0.21 (2)	87 ± 2 (2)	86 ± 4 (2)
PCP	1.6 ± 0.2 (2)	−160 ± 80 (3)	18 ± 10 (3)	0.11 ± 0.02 (3)	72 ± 8 (2)	23 ± 45 (2)
HTX	1.1 ± 0.2 (4)	67 ± 20 (4)	85 ± 9 (4)	0.22 ± 0.15 (4)	83 ± 14 (3)	77 ± 19 (3)

statistically significant difference in the alterations in labeling efficiencies (ANOVA $p = 0.14$). Nonetheless, there were consistently larger reductions at δM2-13 than δM2-9. Consequently, HTX caused statistically significantly changes in the ratios of incorporation in M2-9 to M2-13 in the δ-subunit (0.51, −HTX; 1.1, +HTX, $p \leq 0.001$). There was no significant change in the ratio of incorporation in αM2 ($p = 0.17$).

Discussion

In these studies we examined the effects of tetracaine, PCP, and HTX on the pattern of photolabeling of [^{125}I]TID in the nAChR M2 ion channel domain. Previously [^{125}I]TID and [^{3}H]tetracaine had each been shown by direct photolabeling to bind within the ion channel at the level of M2-9 and M2-13 in the closed state. Our results now demonstrate that tetracaine, the dimethylaminoethyl ester of *p*-butylaminobenzoic acid, which is charged at physiological pH, binds in a mutually exclusive manner with [^{125}I]TID, an uncharged benzene derivative. In contrast, for PCP, a three-ring aromatic tertiary amine, and HTX, a bulky two-ring secondary amine (Fig. 1), we found no evidence for simple, competitive interactions with [^{125}I]TID within the ion channel in the closed state. In the presence of PCP or HTX, there was no evidence that [^{125}I]TID was shifted to another locus within the ion channel domain, because [^{125}I]TID photolabeling was still restricted to amino acids M2-9 and M2-13. In the presence of HTX or especially PCP there was an alteration of the pattern of [^{125}I]TID labeling at M2-9 and M2-13 inconsistent with

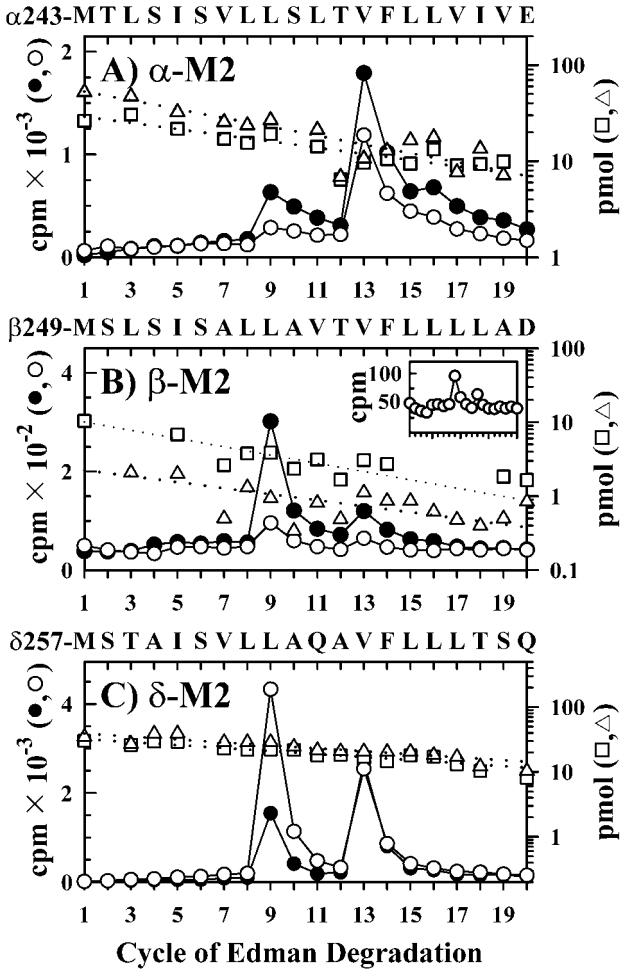

Fig. 6. Effect of PCP on [^{125}I]TID incorporation within the M2 ion channel domain. A–C, ^{125}I (●, ○) and picomoles of residues (□, △) released during N-terminal sequencing of α-, β-, and δ-subunit fragments isolated by SDS-PAGE and reversed phase HPLC from nAChRs photoincorporated with [^{125}I]TID in the absence (●, □) and presence (○, △) of 50 μM PCP. The data for the three subunits are from separate labeling experiments. For each subunit, the primary sequence detected began at the amino terminus of the M2 segment, and that sequence is shown at the top of each panel. No other sequences were detected at >10% of the primary sequence, except for the β-subunit control, which contained a secondary sequence beginning at βLys-216 at the amino terminus of βM1 at one-third the level of the primary sequence. The initial (I_0) and repetitive (R) yields of for each sample as well as the efficiency of incorporation into M2-9 and M2-13 are listed in the Table 1B. Inset, ^{125}I release (○) for the β-subunit sample labeled in the presence of PCP plotted on an expanded scale.

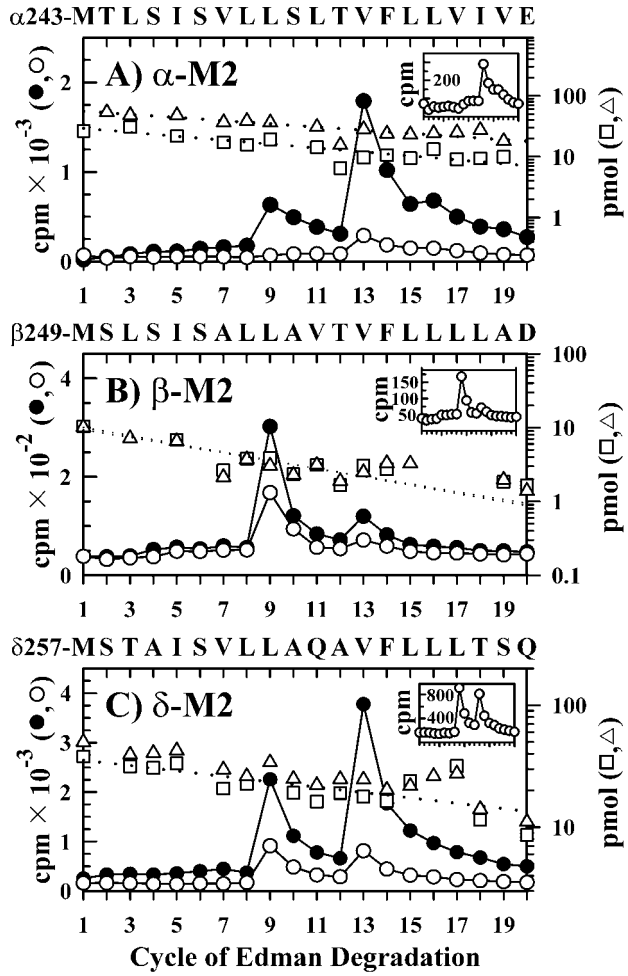

Fig. 7. Effect of HTX on [^{125}I]TID incorporation within the M2 ion channel domain. A–C, ^{125}I (●, ○) and picomoles of residues (□, △) released during N-terminal sequencing of α-, β-, and δ-subunit fragments isolated by SDS-PAGE and reversed phase HPLC from nAChRs photoincorporated with [^{125}I]TID in the absence (●, □) and presence (○, △) of 30 μM HTX. The controls for the α- and β-subunits are the same as in Fig. 6, because for those subunits the labelings with PCP and HTX were carried out in parallel. For each subunit, the primary sequence detected began at the amino terminus of the M2 segment, and that sequence is shown at the top of each panel. No other sequences were detected at >10% of the primary sequence, except for the β-subunit control, which contained a secondary sequence beginning at βLys-216 at the amino terminus of βM1 at one-third the level of the primary sequence. The initial (I_0) and repetitive (R) yields of sequencing as well as the efficiency of incorporation into M2-9 and M2-13 are listed in Table 1C. Insets, ^{125}I release (○) profiles for the samples labeled in the presence of PCP plotted on an expanded scale.

mutually exclusive binding. The simplest interpretation of the data is that in the absence of agonist, PCP, or HTX binds at another site, presumably in the ion channel domain, and the binding results in a subtle shift of the orientation of [^{125}I]TID bound at M2-9/13.

Tetracaine. In the analytical labeling experiments, high concentrations of tetracaine reduced [^{125}I]TID photoincorporation into the nAChR γ-subunit by 92 ± 1% (Fig. 1). This amount of inhibition would be expected for a drug that prevented [^{125}I]TID photolabeling within the M2 ion channel domain either by preventing the binding of [^{125}I]TID or by stabilizing the desensitized state of the nAChR (White and Cohen, 1988; 1992). However, tetracaine at concentrations up to 100 μM does not desensitize the nAChR (Boyd and Cohen, 1984; Middleton et al., 1999), and the IC_{50} value of 3 μM for tetracaine inhibition is consistent with its binding to the M2 ion channel domain in the absence of agonist. In our studies, nonradioactive TID reduced the equilibrium binding of [^{3}H]tetracaine by 95 ± 3%, a result consistent with competitive inhibition, although in view of the uncertainties, noncompetitive inhibition cannot be excluded.

We characterized [^{125}I]TID photoincorporation in the M2 ion channel domain in the absence and presence of 30 μM tetracaine. Sequence analysis through the M2 segments from the α-, β-, and δ-subunits showed that tetracaine reduced the efficiency of labeling at the positions normally labeled by [^{125}I]TID in the absence of tetracaine (M2-9 and M2-13) and did not shift [^{125}I]TID labeling to any other amino acids in the M2 segments. Tetracaine at 30 μM was not expected to produce maximal inhibition of [^{125}I]TID photolabeling. Based upon the IC_{50} value from the analytical photolabeling experiments (Fig. 2), if tetracaine and [^{125}I]TID bound in a formally competitive manner then 30 μM tetracaine would reduce [^{125}I]TID's occupancy of the ion channel by 90% and as a result, there would be a 90% reduction in the labeling at M2-9 and M2-13. Because that is the value seen experimentally (88%), we conclude that the remaining [^{125}I]TID photolabeling at M2-9 and M2-13 originates from the nAChRs that have not bound tetracaine.

PCP and HTX. In the absence of agonist PCP binding to its high-affinity site in the nAChR causes an allosteric inhibition of [^{125}I]TID photolabeling of the α-, β-, and γ-subunits and an increased photolabeling of the δ-subunit (White and Cohen, 1988; Ryan et al., 2001). HTX binding to its high-affinity site causes an allosteric inhibition of [^{125}I]TID photoincorporation into each nAChR subunit (White and Cohen, 1988). In our study, concentrations of PCP (50 μM) and HTX (30 μM) were used that in the previous studies were shown to cause maximal inhibition (or potentiation) of [^{125}I]TID photoincorporation into the nAChR as determined at the level of individual subunits. When we characterized by sequence analysis PCP's or HTX's effects on [^{125}I]TID incorporation in the M2 segments from nAChR α-, β-, and δ-subunits, we found that neither PCP nor HTX resulted in the labeling by [^{125}I]TID of any amino acids within M2 not labeled in the absence of the drugs. PCP (50 μM) *enhanced* the labeling of δM2-9 by 2- to 3-fold and altered the efficiency of [^{125}I]TID incorporation into the other residues by significantly different percentages (Fig. 6; Table 1). Furthermore, the ratios of ^{125}I incorporation in αM2-9 to αM2-13 and δM2-9 to δM2-13 were significantly different from those observed in the absence of PCP (Table 2). This alteration in the pattern of labeling at M2-9/M2-13 suggests that PCP changes the orientation of [^{125}I]TID's diazirine with respect to the labeled residues, a result consistent with an allosteric interaction between PCP and TID. Similarly, the change in the ratio of [^{125}I]TID incorporation in δM2-9 to δM2-13 seen in the presence of HTX indicates that HTX also alters allosterically the structure of the TID binding domain.

Is it possible that PCP or HTX might bind simultaneously with [^{125}I]TID at the level of M2-9/M2-13? We have shown that tetracaine, which by direct photolabeling studies is known to bind in the ion channel at the level of M2-9/M2-13 (Gallagher and Cohen, 1999), inhibits competitively [^{125}I]TID photolabeling in the ion channel. Because tetracaine is a small aromatic amine containing only a single benzene ring, it is highly unlikely that a bulky, three-ringed compound such as PCP could bind within the pore at the level of the TID site and have the effects that it does on [^{125}I]TID labeling of M2-9 and M2-13. The enhancement of [^{125}I]TID photoincorporation at δM2-13 might be rationalized if the binding of PCP shifted [^{125}I]TID toward that position, but there was no evidence that PCP completely shielded [^{125}I]TID from contact with the other residues at M2-9/13. Similarly, it is improbable that HTX, a bulky two-ringed compound, could bind simultaneously with [^{125}I]TID at M2-9/13 and cause only a ~70% allosteric reduction in [^{125}I]TID labeling, whereas the binding of tetracaine and [^{125}I]TID is mutually exclusive. Therefore, we believe that PCP and HTX do not bind at the level of M2-9/M2-13 in the closed channel. In the desensitized nAChR aromatic amines NCAs, including [^{3}H]chlorpromazine and [^{3}H]triphenylmethylphoshponium bind at a site centered at M2-6 (Giraudat et al., 1986, 1987, 1989; Hucho et al., 1986; Revah et al., 1990), whereas [^{3}H]meproadifen mustard seems to bind near M2-20 at the extracellular end of the channel (Pedersen et al., 1992). Although we would be surprised if PCP or HTX binds near M2-6 in the resting state, perhaps either (or both) bind toward the extracellular end of the channel domain. Alternatively, it is possible that they may bind to a site not involving contributions from the M2 segments, as has been suggested for quinacrine in the open channel state (DiPaola et al., 1990).

Because TID and tetracaine label many of the same residues within the M2 segments and interact in a formally competitive manner, it is surprising that PCP and HTX interact allosterically with TID but competitively with tetracaine. In its extended conformation tetracaine is a longer molecule than TID. Perhaps PCP and HTX bind within the ion channel at a site that can overlap with tetracaine, but not TID. We consider it more likely that the ion channel cannot accommodate two compounds that are positively charged (such as PCP and tetracaine or HTX and tetracaine) even though they bind at different levels within the channel. However, the ion channel seems to be able to accommodate two compounds if one is positively charged and one is neutral (such as TID), as long as they bind at different loci within the ion channel.

Because PCP binds with higher affinity to the nAChR in the desensitized state than in the resting state (Heidmann et al., 1983), it is possible that the PCP-induced conformational changes in the [^{125}I]TID binding domain may reflect stabilization by PCP of the nAChR-desensitized state. For nAChRs desensitized by the agonist carbamylcholine, the efficiency of

[^{125}I]TID incorporation in M2-9/13 is reduced by 90%, and there is also labeling at M2-2 and M2-6 that is not seen in the absence of agonist (White and Cohen, 1992). The effects of PCP on [^{125}I]TID photolabeling were clearly different than those of carbamylcholine, but it will be important to also examine the effects of PCP on [^{125}I]TID photoincorporation in the presence of agonist. If the alteration of the pattern of [^{125}I]TID photolabeling we see at M2-9/13 occurs because PCP is shifting the nAChR to the desensitized state, we would expect to see a similar labeling pattern in the presence of agonist. It would also be of interest to determine in the presence of agonist the effects on [^{125}I]TID photolabeling of chlorpromazine or meproadifen, strongly desensitizing NCAs whose binding sites are known.

Given the effects of PCP and HTX on [^{125}I]TID incorporation observed here, it will be of interest to directly identify their binding sites in the closed channel state. Preliminary studies have examined the ability of [^{3}H]HTX and [^{3}H]azido PCP to photoincorporate into the *Torpedo* species nAChR (Oswald and Changeux, 1981; Mosckovitz et al., 1987). Our data indicate that in the closed channel state [^{3}H]HTX and [^{3}H]azido PCP do not bind at the level of M2-9/13, but direct photoaffinity labeling studies will be required to determine where they do bind.

References

Arias HR (1998) Binding sites for exogenous and endogenous non-competitive inhibitors of the nicotinic acetylcholine receptor. *BBA Rev Biomembr* **1376:**173–220.

Blanton MP and Cohen JB (1992) Mapping the lipid exposed regions in the *Torpedo* species nicotinic acetylcholine receptor. *Biochemistry* **31:**3738–3750.

Blanton MP and Cohen JB (1994) Identifying the lipid-protein interface of the *Torpedo* nicotinic acetylcholine receptor: secondary structure implications. *Biochemistry* **33:**2859–2872.

Blanton MP, Dangott LJ, Raja SK, Lala AK and Cohen JB (1998) Probing the structure of the nicotinic acetylcholine receptor ion channel with the uncharged photoactivatable compound [^{3}H]diazofluorene. *J Biol Chem* **273:**8659–8668.

Boyd ND and Cohen JB (1984) Desensitization of membrane-bound *Torpedo* acetylcholine receptor by amine noncompetitive antagonists and aliphatic alcohols: studies of [^{3}H]-acetylcholine binding and $^{22}Na^{+}$ ion fluxes. *Biochemistry* **23:**4023–4033.

Brunner J and Semenza G (1981) Selective labeling of the hydrophobic core of membranes with 3-(trifluoromethyl)-3-m-([^{125}I]iodophenyl)diazirine, a carbene-generating reagent. *Biochemistry* **20:**7174–7182.

Charnet P, Labarca C, Leonard RJ, Vogelaar NJ, Czyzyk L, Gavin A, Davidsen N and Lester HA (1990) An open-channel blocker interacts with adjacent turns of α-helices in the nicotinic acetylcholine receptor. *Neuron* **2:**87–95.

Cleveland DW, Fischer SG, Kirschner MW and Laemmli UK (1977) Peptide mapping by limited proteolysis in sodium dodecyl sulfate and analysis by gel electrophoresis. *J Biol Chem* **252:**1102–1106.

Corringer P-J, Le Novere N and Changeux J-P (2000) Nicotinic receptors at the amino acid level. *Annu Rev Pharmacol Toxicol* **40:**431–458.

DiPaola M, Kao PN and Karlin A (1990) Mapping the α-subunit site photolabeled by the noncompetitive inhibitor [^{3}H]quinacrine azide in the active state of the nicotonic acetylcholine receptor. *J Biol Chem* **265:**11017–11029.

Dreyer EB, Hasan F, Cohen SG and Cohen JB (1986) Reaction of [^{3}H]-meproadifen mustard with membrane-bound acetylcholine receptor. *J Biol Chem* **261:**13727–13734.

Eaton MJ, Labarca C and Eterovic VA (2000) M2 Mutations of the nicotinic acetylcholine receptor increase the potency of the non-competitive inhibitor phencyclidine. *J Neurosci Res* **61:**44–51.

Gallagher MJ and Cohen JB (1999) Identification of amino acids of the *Torpedo* nicotinic acetylcholine receptor contributing to the binding site for the noncompetitive antagonist [^{3}H]tetracaine. *Mol Pharmacol* **56:**300–307.

Giraudat J, Dennis M, Heidmann T, Chang J-Y and Changeux J-P (1986) Structure of the high-affinity binding site for noncompetitive blockers of the acetylcholine receptor: serine-262 of the δ subunit is labeled by [^{3}H]chlorpromazine. *Proc Natl Acad Sci USA* **83:**2719–2723.

Giraudat J, Dennis M, Heidmann T, Haumont P-Y, Lederer F and Changeux J-P (1987) Structure of the high-affinity binding site for noncompetitive blockers of the acetylcholine receptor: [^{3}H]chlorpromazine labels homologous residues in the β and γ chains. *Biochemistry* **26:**2410–2418.

Giraudat J, Gali J-Z, Revah F, Changeux J-P, Haumont P-Y and Lederer F (1989) The noncompetitive blocker [^{3}H]chlorpromazine labels segment M2 but not segment M1 of the nicotinic acetylcholine receptor α-subunit. *FEBS Letts* **253:**190–198.

Heidmann T, Oswald RE and Changeux J-P (1983) Multiple sites of action for noncompetitive blockers on acetylcholine receptor rich membrane fragments from. *Torpedo marmorata. Biochemistry* **22:**3112–3127.

Hucho F, Oberthur W and Lottspeich F (1986) The ion channel of the nicotinic acetylcholine receptor is formed by the homologous helices M II of the receptor subunits. *FEBS Letts* **205:**137–142.

Hucho F, Tsetlin VI and Machold J (1996) The emerging three-dimensional structure of a receptor - the nicotinic acetylcholine receptor. *Eur J Biochem* **239:**539–557.

Imoto K, Busch C, Sakmann B, Mishina M, Konno T, Nakai J, Bujo H, Mori Y, Fukuda K and Numa S (1988) Rings of negatively charged amino acids determine the acetylcholine receptor channel conductance. *Nature (Lond)* **335:**645–648.

Imoto K, Konno T, Nakai J, Wang F, Mishina M and Numa S (1991) A ring of uncharged polar amino acids as a component of channel constriction in the nicotinic acetylcholine receptor. *FEBS Letts* **289:**193–200.

Middleton RE, Strnad NP and Cohen JB (1999) Photoaffinity labeling the Torpedo nicotinic acetylcholine receptor with [^{3}H]tetracaine, a nondesensitizing noncompetitive antagonist. *Mol Pharmacol* **56:**290–299.

Mosckovitz R, Haring R, Gershoni J, Kloog Y and Sokolovsky M (1987) Localization of azidophencyclidine-binding site on the nicotinic acetylcholine receptor α-subunit. *Biochem Biophys Res Commun* **145:**810–816.

Oswald RE and Changeux J-P (1981) Ultraviolet light-induced labeling by noncompetitive blockers of the acetylcholine receptor from *Torpedo marmorata. Proc Natl Acad Sci USA* **78:**3925–3929.

Pedersen SE, Dreyer EB and Cohen JB (1986) Location of ligand binding sites on the nicotinic acetylcholine receptor α-subunit. *J Biol Chem* **261:**13735–13743.

Pedersen SE, Sharp SD, Liu W-S and Cohen JB (1992) Structure of the noncompetitive antagonist binding site in the *Torpedo* nicotinic acetylcholine receptor: [^{3}H]meproadifen mustard reacts selectively with α-subunit Glu-262. *J Biol Chem* **267:**10489–10499.

Revah F, Galzi JL, Giraudat J, Haumont P-Y, Lederer F and Changeux J-P (1990) The noncompetitive blocker [^{3}H]chlorpromazine labels three amino acids of the acetylcholine receptor γ subunit: implications for the α-helical organization of regions MII and for the structure of the ion channel. *Proc Natl Acad Sci USA* **87:**4675–4679.

Ryan SE, Blanton MP and Baenziger JE (2001) A conformational intermediate between the resting and desensitized states of the nicotinic acetylcholine receptor. *J Biol Chem* **276:**4796–4803.

Schagger H and von Jagow G (1987) Tricine-sodium dodecyl sulfate-polyacrylamide gel electrophoresis for the separation of proteins in the range from 1 to 100 KDa. *Anal Biochem* **166:**368–379.

Tamamizu S, Todd AP and McNamee MG (1995) Mutations in the M1 region of the nicotinic acetylcholine receptor alter the sensitivity to inhibition by quinacrine. *Cell Mol Neurobiol* **15:**427–438.

White BH and Cohen JB (1988) Photolabeling of membrane-bound *Torpedo* nicotinic acetylcholine receptor with the hydrophobic probe 3-trifluoromethyl-3-(m-[^{125}I]iodophenyl)diazirine. *Biochemistry* **27:**8741–8751.

White BH and Cohen JB (1992) Agonist-induced changes in the structure of the acetylcholine receptor M2 regions revealed by photoincorporation of an uncharged nicotinic non-competitive antagonist. *J Biol Chem* **267:**15770–15783.

White BH, Howard S, Cohen SG and Cohen JB (1991) The hydrophobic photoreagent 3-(trifluoromethyl)-3-(m-[^{125}I]iodophenyl)diazirine is a novel noncompetitive antagonist of the nicotinic acetylcholine receptor. *J Biol Chem* **266:**21595–21607.

Zhang H and Karlin A (1997) Identification of acetylcholine receptor channel-lining residues in the M1 segment of the beta-subunit. *Biochemistry* **36:**15856–15864

Send reprint requests to: Jonathan B. Cohen, Department of Neurobiology, Harvard Medical School, 220 Longwood Ave., Boston, MA 02115. E-mail: jonathan_cohen@hms.harvard.edu